Indian Journal of Geo Marine Sciences
Vol. 53 (05), May 2024, pp. 384-397
DOI: 10.56042/ijms.v53i05.21671

Modelling ocean diurnal cycle and its scale interaction to longer scale climatic variabilities

M Pradhan[a,*], S A Rao[a] & A Bhattacharya[b]

[a]Monsoon Mission, Indian Institute of Tropical Meteorology, Pune, Maharashtra – 411 008, India

[b]Department of Applied Mechanics, Indian Institute of Technology, Delhi – 110 016, India

*[E-mail: maheswar@tropmet.res.in]

Received 29 March 2024; revised 28 May 2024

Coupled climate models play a crucial role in weather and climate prediction/projection at different temporal (diurnal, intra-seasonal, seasonal, etc.) and spatial (short-range, extended-range, long-range) scales. Although coupled models have come a long way in their development, several challenges remain unaddressed, such as (a) underestimation of diurnal phase and amplitude in ocean and atmospheric parameters, (b) misrepresentation of phase and amplitude of intra-seasonal variability and feedbacks, and (c) high seasonal mean biases in air-sea interactive properties and precipitation, that hinders the weather and climate forecasts at various temporal and spatial scales. The present article documents these coupled modelling problems and explores a possible approach to address these issues. This study shows that representing the diurnal ocean skin temperature variability can be a way forward to overcome the long-lasting diurnal, intra-seasonal, and seasonal scale problems specifically linked to the Indian summer monsoon period. Through carefully designed sensitivity experiments, this study shows that the implementation of a diurnal skin temperature parameterisation along with a modern turbulent bulk flux algorithm improves the diurnal variability of surface ocean, subsurface ocean, and atmospheric convection. The diurnal improvements then scale interacts with longer range variabilities and also improves the representation of intra-seasonal and seasonal variabilities in a coupled climate model.

[**Keywords**: Bulk flux parameterisation, Diurnal cycle, Indian summer monsoon, Monsoon intra-seasonal oscillation, Rectification, Skin temperature]

Introduction

During the last few decades, the application of coupled climate models has increased beyond predicting weather and climate to the early warning system and managing agriculture, fisheries, electricity, water resources, etc. The forecasting systems are progressively improving by improving model resolution[1–3], physics[4–7], and data assimilation[8–11]. However, there are still challenges in using coupled models as forecasting or prediction tools. At the diurnal scale, studies have reported that coupled models underestimate the amplitude of diurnal precipitation over tropical lands and oceans. There are two major problems with the climate models in simulating the diurnal precipitation: (a) the precipitation over the land and oceans occurs much earlier in models than in reality, and (b) the diurnal amplitude or range of precipitation is significantly underestimated in models. Several attempts have been made by researchers and model developers across the globe to overcome these challenges. For example, Chakraborty & Krishnamurti[12] attempted to improve the diurnal cycle of tropical precipitation by implementing a unified cloud parameterisation scheme, which is a multi-model super ensemble technique of taking advantage of different cloud parameterisation schemes available in the climate models. Ganai *et al.*[4] implemented a Revised Simplified Arakawa-Schubert (RSAS) convective parameterisation scheme in the Climate Forecast System (CFS) model to improve the diurnal characteristics of precipitation. Xie *et al.*[13] have revised the convective triggering function in Energy's Energy Exascale Earth System Model (E3SM) to improve tropical precipitation's diurnal phase and amplitude. Most of these studies have shown improvements in phase or timing of diurnal precipitation. However, the improvement in the diurnal amplitude of precipitation has not been very exciting. On the other hand, Dai & Trenberth[14] suggested that a weaker diurnal cycle in convective precipitation in the Community Climate System Model (CCSM) is mainly due to a lack of diurnal variation in Sea Surface Temperature (SST). Chen &

Houze[15] have shown that the diurnal sea surface warming provides the conditions needed for tropical convection over the Indo-Pacific oceanic regions. Therefore, forecasting diurnal extreme precipitations is difficult using coupled climate models. Similarly, the phase and amplitude of intra-seasonal variabilities, such as the Monsoon Intra-Seasonal Oscillation (MISO) and Madden Julian Oscillation (MJO), are also not well represented in coupled model simulations. The phase speed of intra-seasonal variability in most of the coupled models is found to be slower than observation[16]. On the other hand, the amplitude of intra-seasonal variabilities is underestimated in the present-generation models[17]. The inability of the models to simulate intra-seasonal variability comes from the poor representation of air-sea interaction in coupled models[16,17]. The mean state bias in air-sea interaction can hinder the phase and amplitude simulations during the MJO life cycle[18]. At the seasonal scale, the dry (wet) precipitation bias over the tropical landmasses (oceans) is also reported in many of the earlier works[19,20]. Earlier studies have linked precipitation biases to the coupled models' SST biases. Pillai *et al*.[21,22] and Pradhan *et al*.[23] have suggested that the models with large (small) cold SST bias over the equatorial central Pacific have larger (smaller) dry bias over the Indian landmass. Also, studies like Pradhan *et al.*[24] have shown that the wrong SST and Indian Summer Monsoon Rainfall (ISMR) relation over the tropical Pacific and Indian Ocean are also due to misrepresentation of air-sea boundary characteristics such as the SST-flux relation, SST-thermocline relation, etc.

In this study, an attempt has been made to address the multi-scale (diurnal to seasonal) biases and misrepresentation of teleconnections associated with the Indian summer monsoon by improving the air-sea interaction in coupled models. In coupled models, the ocean and atmosphere interact by exchanging turbulent fluxes such as momentum (wind stress) and heat (latent heat, sensible heat, shortwave, and longwave radiations). This noble approach involves modifying the existing surface flux parameterisation algorithm and implementing a skin temperature parameterisation scheme. The air-sea interactive flux feedbacks govern the life cycle of most of the known climate variabilities such as the El Niño, La Niña, and Southern Oscillation (ENSO[25]), Indian Ocean Dipole (IOD[26,27]), Madden Julian Oscillation (MJO[18,28]), etc. Therefore, better qualitative and quantitative representation of surface momentum and heat fluxes is required for better predictability at different temporal and spatial scales. In coupled models, the turbulent fluxes are computed following bulk flux algorithms, and the computed fluxes are sensitive to the choice of bulk flux scheme used[29].

As mentioned earlier, the turbulent fluxes at the air-sea interface are one component of ocean-atmospheric boundary conditions, and their misrepresentation leads to model simulation problems on a diurnal to seasonal scale. Another important aspect of air-sea interaction is representing the true ocean skin temperature rather than using the bulk ocean temperature as the SST. The estimation of surface fluxes, such as the latent heat flux, sensible heat flux, and wind stress, directly or indirectly depends on the ocean skin temperature. Hence, the accuracy of surface fluxes also depends on the accuracy in representing the true ocean skin temperature. However, most coupled models use the 5 m temperature as the boundary forcing from the ocean to the atmospheric model. The 5 m ocean temperature misses two crucial diurnal processes that clearly distinguish between bulk and skin temperature. First, the daytime warming is due to the establishment of a diurnal warm layer as the surface ocean absorbs incoming solar radiation. Second is the night time cooling at the ocean surface due to outgoing longwave radiation, latent heat, and sensible heat from the air-sea interface. Due to the diurnal warming, the ocean skin temperature remains warmer than the bulk temperature during the daytime, whereas, due to the night time cooling, the ocean skin remains cooler than the bulk oceanic temperature. A schematic representation of diurnal warming and cooling is given in Figure 1. Diurnal ocean variability is shown to reduce the errors in simulated SST and upper ocean temperature profiles by 5 – 40 % and 10 – 40 %, respectively, in the Bay of Bengal (BoB)[30]. The cold tongue biases over the equatorial Pacific region are also reduced with diurnal skin temperature parameterisation[31]. The cool skin effect has also been shown to reduce errors associated with the overestimation of heat flux[32].

In this direction, the coupled model, the Climate Forecast System (CFS), is used as the tool to investigate the role of diurnal skin temperature and flux parameterisation on various temporal and spatial scale ocean and atmospheric processes. Dynamical long-range prediction for the Indian monsoon is based on Monsoon Mission CFS (MMCFS[33]) with increased atmospheric horizontal resolution (T382; 38 km) in CFSv2[(ref. 34)] and has been operational at India Meteorological Department (IMD) since 2012. The default version of CFS uses the National Center for Atmospheric Research (NCAR) flux[35] scheme to estimate the air-sea interaction fluxes. Earlier studies[36,37] have highlighted that the flux scheme, such as the Coupled-Ocean Atmosphere Response Experiment (COARE) 3.0[(refs. 38,39)] performs better than the NCAR flux scheme. COARE 3.0 is one of the popular bulk flux algorithms used by oceanographers to estimate turbulent fluxes for its efficiency and accuracy. One of the major advantages of COARE 3.0 is the presence of diurnal skin temperature parameterisation, which the NCAR flux scheme or the default CFS model lacks. Therefore, the present study attempts to resolve some of the long-standing coupled model problems that exist at various temporal and spatial scales. In this direction, sensitivity experiments are carried out using the CFS model (a) without diurnal skin temperature and with NCAR flux parameterisation, and (b) with diurnal skin temperature and with COARE 3.0 flux parameterisation.

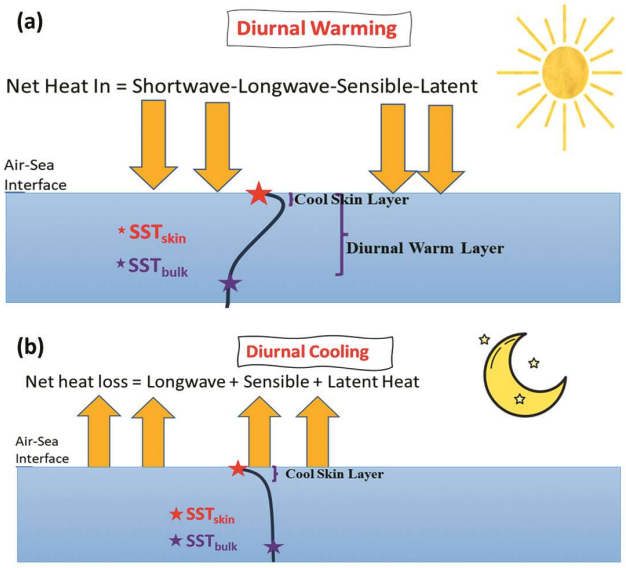

Fig. 1 — Schematic representation of the processes involved in (a) Diurnal warming, and (b) Diurnal cooling of ocean skin as compared to the bulk temperature

Materials and Methods

Data: Observation and model

As mentioned above, the study investigates whether the novel approach of revising flux and skin temperature parameterisation helps overcome model biases at diurnal to seasonal time scales. Unless explicitly mentioned, this study focuses on model biases during the boreal summer season, *i.e.*, from June to September (JJAS) months. The details, including the source of data, its temporal and spatial resolutions, and references for the observation/reanalysis datasets used in the analyses, are reported in Table 1.

The present study uses the CFS version 2 (CFSv2) model as the experimental tool, and its coupled configuration is represented in Figure 2. NCEP-Climate Forecast System Reanalysis (CFSR[40]), atmospheric and oceanic initial conditions are used to initialise the model during February month and are integrated for nine months. The model hindcasts (for a period of 1998 – 2017) are prepared by following the lagged ensemble method where the model is initialised with ten ensemble members on the 5th, 10th, 15th, 20th, and 25th February at 00 and 12 UTC of each

Table 1 — Details of different observation/reanalysis data used in this study

Dataset[Reference]	Variables	Time Period	Resolution	
			Temporal	Spatial
SeaFlux[54]	SST	1998-2008	Hourly	0.25°×0.25°
TRMM[55]	Rainfall	1998-2017	3-Hourly	0.25°×0.25°
TAO/TRITON RAMA[56]	Subsurface Temperature	1998-2017	Hourly	Point Obs.
GPCP v2.3[57]	Rainfall	1981-2017	Monthly	2.5°×2.5°
ERSST[58]	SST	1981-2017	Monthly	2.5°×2.5°
TropFlux[59]	LHF, SHF, WS	1998-2015	Daily	1.0°×1.0°
JRA55[60]	Atmospheric Variables	1981-2017	Daily	1.25°×1.25°
GLORYS[61]	MLD	1998-2008	Daily	1/12°

year. In the present study, the CFSv2 is used at a lower horizontal resolution of the atmospheric model (T126; 100 km) due to limited computational resources to carry out the sensitivity experiments. MOM4p0 is the ocean model with a varying meridional resolution (0.25° at lower latitude to progressively decreasing to 0.5° at higher latitude) and fixed zonal resolution (0.5°). The ocean and atmospheric model time step is set to 30 and 10 min, respectively, and they interact with each other at every 30-minute interval (coupling time). In the default (control run: CTL) configuration, the 5 m ocean temperature is passed from the ocean model to the atmospheric model as a boundary forcing, and the bottom atmospheric meteorological parameters (winds, humidity, pressure, etc.) and surface fluxes (latent heat, sensible heat, wind stress, long wave, and shortwave radiation) are passed from the atmosphere model to the ocean model as a forcing. However, with the implementation of skin temperature and COARE 3.0 flux parameterisation, the boundary forcing to both the ocean and atmospheric models are modified at each coupling time step. In the revised (sensitivity run: SEN) model configuration, the corrected skin temperature is passed from the ocean model to the atmosphere model and the COARE 3.0 estimated surface fluxes from the atmosphere model to the ocean model as forcing.

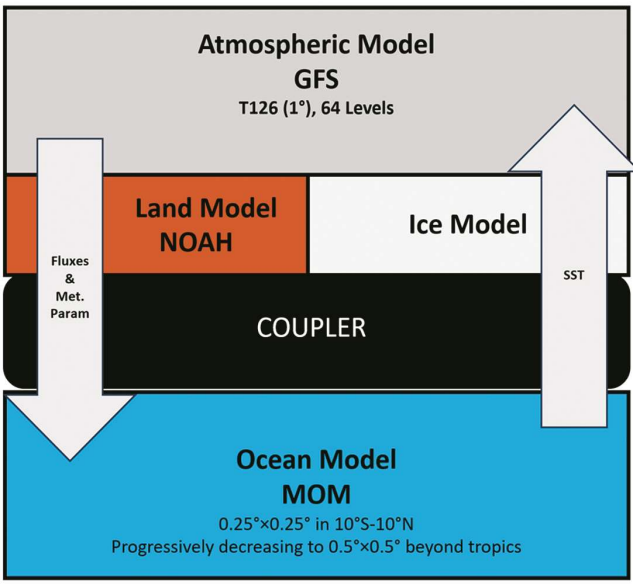

Fig. 2 — Schematic representation of various components of the CFSv2 model

Results

Addressing the diurnal scale problems

As mentioned earlier, the SEN and CTL hindcast runs differ from each other in terms of the representation of skin temperature variability. The impact of representing skin temperature on the diurnal variability of SST can be seen in Figure 3, where a diurnal range of SST (dsst) is compared in two model simulations against the observation for the three

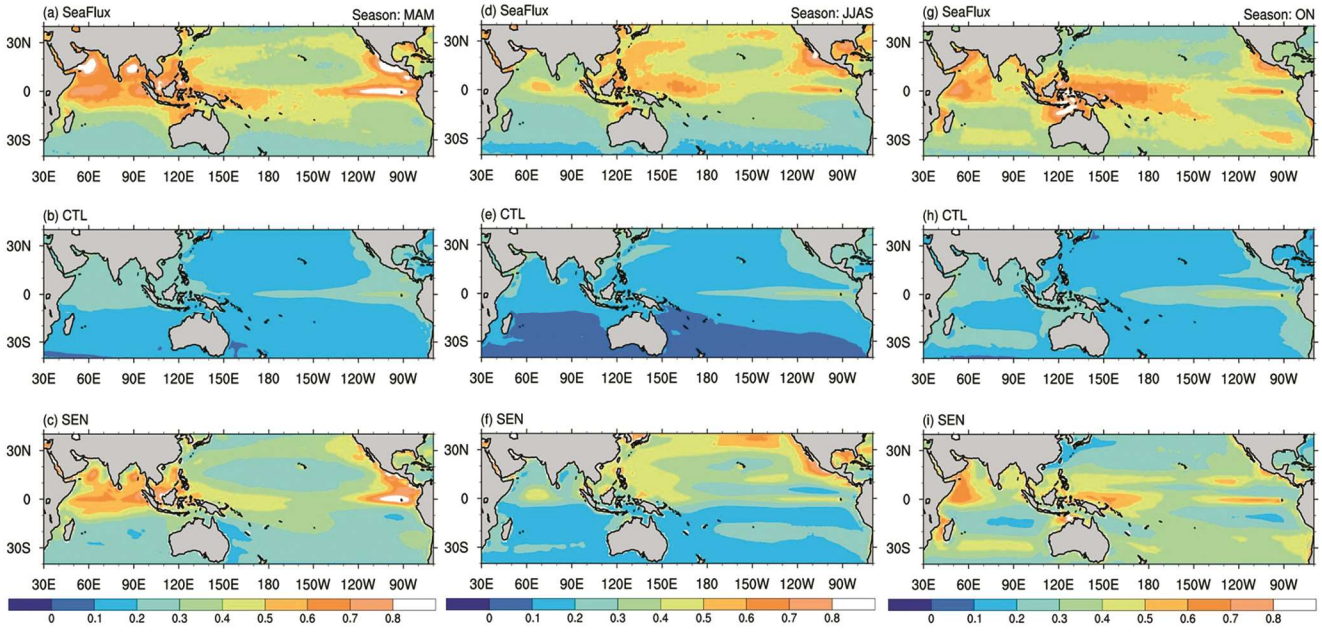

Fig. 3 — Three months (March to May) mean diurnal range in SST (dsst; °C) from (a) Observation (Sea-flux), (b) CTL, and (c) SEN run. (d - f) and (g - i) are the same as (a - c) but mean during the months of June – September and October – November (ON)

seasons (i) March to May (MAM), (ii) June to September (JJAS), and (iii) October to November (ON). The diurnal range is computed as the maximum minus minimum temperature difference during a 24-hour cycle. For a given season, the mean diurnal range is computed by taking an average of diurnal ranges of each day of the season. The diurnal ocean warming is dependent on solar insolation, wind conditions, and cloud cover. Therefore, the observed diurnal warming is higher (lower) in the summer (winter) hemisphere. During MAM, the tropical Indian Ocean has higher diurnal warming (with a magnitude of 0.8 °C or more) over most of the regions. On the other hand, higher dsst (with a magnitude of 0.8 °C or more) can be seen over relatively smaller regions such as the western and eastern equatorial Pacific Ocean. However, during JJAS, the northern tropical Pacific Ocean (0.6 °C) has a higher magnitude of dsst than the Indian Ocean. Relatively weaker (0.3 – 0.5 °C) diurnal warming can be seen over the equatorial Indian Ocean. During the ON months, the observed diurnal range is comparable in both oceans. The diurnal range in SST is significantly underestimated in the CTL run during all the seasons, as shown in Figure 3(b, e & h), where the seasonal mean maximum dsst reaches 0.3 – 0.4 °C across all the seasons. With the inclusion of diurnal skin temperature parameterisation, the diurnal SST is significantly improved over the tropical Indian Ocean and Pacific Oceans. The magnitude and locations of maximum dsst in the SEN run are comparable and agree better with the observation than that in the CTL run. Over the north and south Pacific Ocean, dsst is still underestimated in the SEN run specifically during the JJAS and ON seasons. This could be attributed to the biases in the horizontal advection of heat and also the biases in shortwave radiation linked to the misrepresentation of stratus clouds in the atmospheric model[23]. Implementing diurnal skin temperature parameterisation helped improve the diurnal variability of the surface ocean, thereby increasing the diurnal range in ocean temperature. Further investigation is carried out on the diurnal SST variability w.r.t the local solar cycle over the BoB and Pacific Ocean, focusing on the boreal summer monsoon period (JJAS). Table 2 shows the diurnal amplitude (local maximum minus local minimum during the local solar cycle) and the maximum and minimum ocean temperature timing at the mentioned locations during the southwest monsoon season. For this analysis, the moored buoy observations are taken as the reference for comparison. From the observed statistic, it can be seen that diurnal amplitude is higher at the Pacific locations (5° N – 156° E, 8° N – 137° E) than at the northern BoB location (15° N – 90° E). Smaller diurnal variability over BoB is due to the strong winds persisting throughout the monsoon season. At these locations, the local solar time for minima and maxima are 7:00 and 15:00 h, respectively. Due to a lack of solar insolation during the night time and a well-mixed layer during the early morning, the surface temperature is minimal. During the local afternoon time, due to the absorption of solar radiation, the surface ocean heats up and achieves a maximum in SST during 15:00 h. However, the timing of minima and maxima is incorrect in the CTL run for all the locations as it achieves the minima and maxima 2 h later than that in observation. The CTL simulated diurnal amplitude is also smaller for these locations. For the Pacific and BoB locations, the underestimation of diurnal amplitude in the CTL run is approximately 50 % and 20 % of the observed magnitude. Interestingly, with the implementation of skin temperature corrections, the diurnal variability in the SEN run has improved significantly, considering both the amplitude and time of maxima/minima. As shown in Table 2, the SEN run could produce the time of diurnal minima (6:00 h) and maxima (15:00 h) correctly over the BoB and Pacific Ocean locations. Also, the diurnal amplitude of SST in SEN over the

Table 2 — Details of the Local Solar Cycle (LSC) in SST computed from moored buoy observations and model simulations during the southwest monsoon season (JJAS)

Location	Observation			CTL			SEN		
	Time of max. (in h)	Time of min.(in h)	Diurnal amplitude (in °C)	Time of max. (in h)	Time of min. (in h)	Diurnal Amplitude (in °C)	Time of max.(in h)	Time of min.(in h)	Diurnal amplitude (in °C)
15° N - 90° E	15	7	0.1597	18	9	0.1304	15	6	0.2056
8° N - 137° E	15	7	0.3349	18	9	0.1707	15	6	0.4498
5° N - 156° E	15	7	0.3538	18	9	0.1444	15	6	0.372

Pacific Ocean and BoB has increased by 150 % (35 %) and 50 % (30 %) as compared to that in the CTL run (OBS), respectively. The revised ocean skin and flux parameterisation not only improves the diurnal surface ocean variability but also improves mixed layer processes in the model simulation. Similar to the previous analysis, further analysis on diurnal amplitude and time of maximum and minimum in Mixed Layer Depth (MLD) is also carried out (Figure not shown). The analysis suggests that the CTL underestimates the depth of the mixed layer, specifically during the night time, compared to the SEN run and observation. The diurnal amplitude calculated in terms of a difference in night time deepening and afternoon shallowing of mixed layer also suggested that the CTL run could not simulate the diurnal amplitude properly over the tropical oceans. Therefore, the impact of skin temperature and flux parameterisation improves the mixed layer processes in addition to the surface ocean energetics.

As mentioned earlier, most of the coupled models have challenges in simulating the diurnal amplitude of tropical precipitation. Therefore, this study analyses the diurnal amplitude of precipitation to show the impact of the surface ocean's diurnal cycle on the diurnal precipitation. Figure 4 shows the diurnal amplitude of precipitation (dprate) calculated as the maximum minus minimum in precipitation during a 24-hour cycle. In observation, the pattern in the diurnal precipitation amplitude resembles that of the seasonal rainfall pattern during JJAS. A high magnitude of diurnal precipitation (~2 – 2.5 mm/hr) can be seen over equatorial Indo-Pacific Oceans and tropical landmasses, including India, Africa, and America. On comparing the model simulations against the observation, it can be seen that although the pattern looks similar to the observation, the magnitude of diurnal amplitude is significantly underestimated in the CTL run. In the presence of diurnal skin temperature variability, the diurnal precipitation amplitude is significantly enhanced and is comparable to the observed pattern and magnitude. However, the SEN run overestimates the diurnal range in precipitation over tropical lands and oceans. The enhancement in dprate in SEN run compared to the CTL run is as high as 1 mm/hr. This analysis's results align with some of the suggestions reported in earlier studies. For example, Slingo[41] suggested the possibility of diurnal SST warming, which can act as a trigger for convection, mostly during the suppressed phase of convection. The triggering can result in the formation of cumulus congestus clouds, which gradually moisten the free atmosphere and generate a favourable condition for deep convection. Also, there is a possibility of an increase in low and mid-level clouds due to the revised COARE 3.0 surface turbulent flux algorithm[42]. Li *et al.*[43] also reported that the forcing due to skin temperature can increase diurnal precipitation over the tropical Indo-Pacific Ocean in an atmospheric model. The above analyses show that an improvement in diurnal surface and mixed-layer oceanic processes can lead to an improvement in diurnal convection and precipitation.

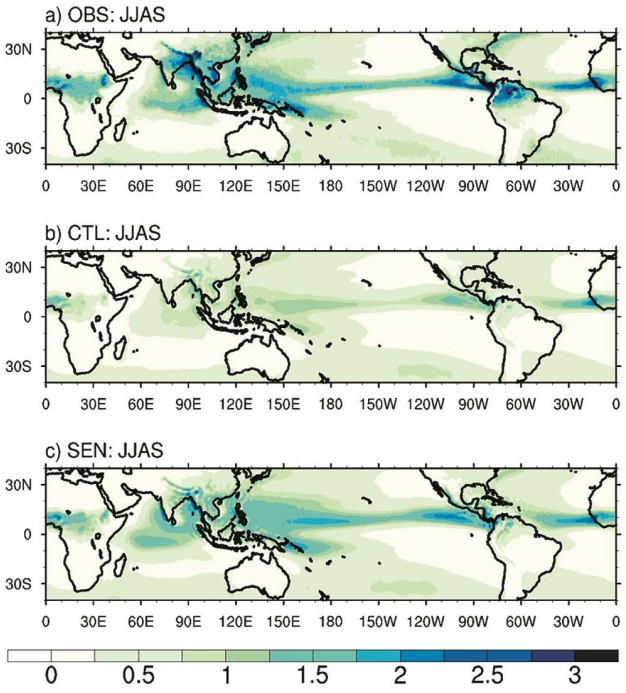

Fig. 4 — Seasonal mean (JJAS) diurnal range in precipitation (dprate; mm/hr) from (a) Observation (TRMM), (b) CTL, and (c) SEN run

Addressing the intra-seasonal problems

Any error present at the diurnal scale can hinder the predictability of longer-time scale variability as the errors grow into longer-time scales via scale interaction. Similarly, the improvements in diurnal time scale can also scale interact and improve the simulation of longer time scale processes in coupled models. Also, studies[44–47] has reported that the diurnal cycle of SST can modulate the atmospheric and oceanic processes at intra-seasonal and seasonal time scales. Therefore, the present section analyse the importance of diurnal SST in improving the

simulation of intra-seasonal variability of SST and monsoon precipitation.

The process of enhancement or reduction in the intra-seasonal SST variability by diurnal variability is called rectification[45,48]. To quantify the amplitude of intra-seasonal rectification of SST by the diurnal SSTs, an index is defined as:

$$Amplitude\ of\ Rectification = \left(SD_{dsst} - SD_{fsst}\right)/ SD_{dsst} \times 100 \quad \ldots (1)$$

Here, SD_{dsst} is the intra-seasonal standard deviation of SST, including the diurnal cycle and SD_{fsst} is the intra-seasonal standard deviation of SST removing diurnal cycle (otherwise known as foundation SST, which is independent of a diurnal cycle). The foundation temperature is taken as the night time minimum temperature[48]. The intra-seasonal signal from both the time series is obtained by applying a 30 – 60-day Lanczos bandpass filter. At various tropical moored buoy locations, the amplitude of rectification is computed from observation and model simulation and is tabulated in Table 3. Although the analysis is performed for all the buoys having continuous (at least for five years) high-frequency (hourly) data, only a few are listed here, and inferences for others can similarly be drawn. Diurnal SST tends to enhance the intra-seasonal variability at most Indo-Pacific Ocean locations except at a few locations over the central and eastern Pacific Ocean. Over the Indo-Pacific warm pool locations (at 137°, 147°, 156°, and 165°), the amplitude of rectification is significantly higher than that of the rest of the locations. At location such as 5° N – 235° E, the observed amplitude of rectification is negative. The enhancement or reduction of intra-seasonal SST variability due to diurnal variability depends on the local ocean and atmospheric feedback[48]. The atmosphere forces the ocean over the Indo-Pacific warm pool region at an intra-seasonal time scale. In this situation, during the suppressed (active) phase of convection, calm (strong) wind conditions are accompanied by high (low) diurnal warming and high (low) intra-seasonal SST warming. Therefore, the dsst-wind and SST-wind relations are out-of-phase, whereas the dsst-SST relation is in phase. On the other hand, over the central and eastern Pacific region, the ocean forces the atmosphere. In this situation, the warm (cool) phase of SST leads to strong (weak) wind conditions, which results in weaker (stronger) diurnal warming. Therefore, the dsst-wind and dsst-SST relations are out of phase with each other, whereas the SST-wind relation is out of phase. Therefore, the observed intra-seasonal rectification is positive over the Indo-Pacific warm pool region and is negative over the eastern Pacific region. On comparing the model simulated values against the observation, the CTL significantly underestimate the rectification amplitude at most locations. In observation, the amplitude is 8 – 12 %, whereas, in CTL run, the amplitude is merely as high as 1 %. With the implementation of diurnal skin temperature variability and its rectification into an intra-seasonal scale, the SEN run produces a realistic amplitude of rectification, as shown in the table. In the SEN run, the simulated amplitude is as high as 10 – 11 % and is comparable to the observed values. Therefore, the above discussion showcased how the inclusion of the diurnal cycle of the ocean can improve the intra-seasonal ocean variability through the process called rectification.

Table 3 — The amplitude of intra-seasonal rectification in observation and model simulation during the southwest monsoon season (JJAS)

Lat (°N)	Lon (°E)	OBS	CTL	SEN
8	90	17.52	1.01	4.81
5	137	12.98	1.10	10.45
5	147	5.71	1.12	8.69
5	156	8.64	1.20	10.74
5	165	8.57	-0.06	4.73
5	180	1.29	0.29	0.65
5	205	3.13	-0.28	-1.05
5	220	-0.10	-0.56	-1.80
5	235	2.96	0.09	0.22

The ocean dynamics over BoB play an important role in governing the monsoon rainfall at diurnal, intra-seasonal, and seasonal time scales. Mujumdar *et al.*[49] have shown that intra-seasonal variability of ocean temperature and mixed layer over BoB can be high despite persistent strong winds during the monsoon season. Earlier studies[16,17] suggested misrepresentation in air-sea interaction over BoB as one reason for improper phase and amplitude of Monsoon Intra-Seasonal Variability (MISO) in coupled models. Therefore, an analysis is carried out to see if the simulation characteristics of MISOs can be improved by improving the SST and turbulent flux representation. For this analysis, MISOs are defined w.r.t. an index calculated by standardised filtered (20 – 90-day Lanczos bandpass filter) rainfall

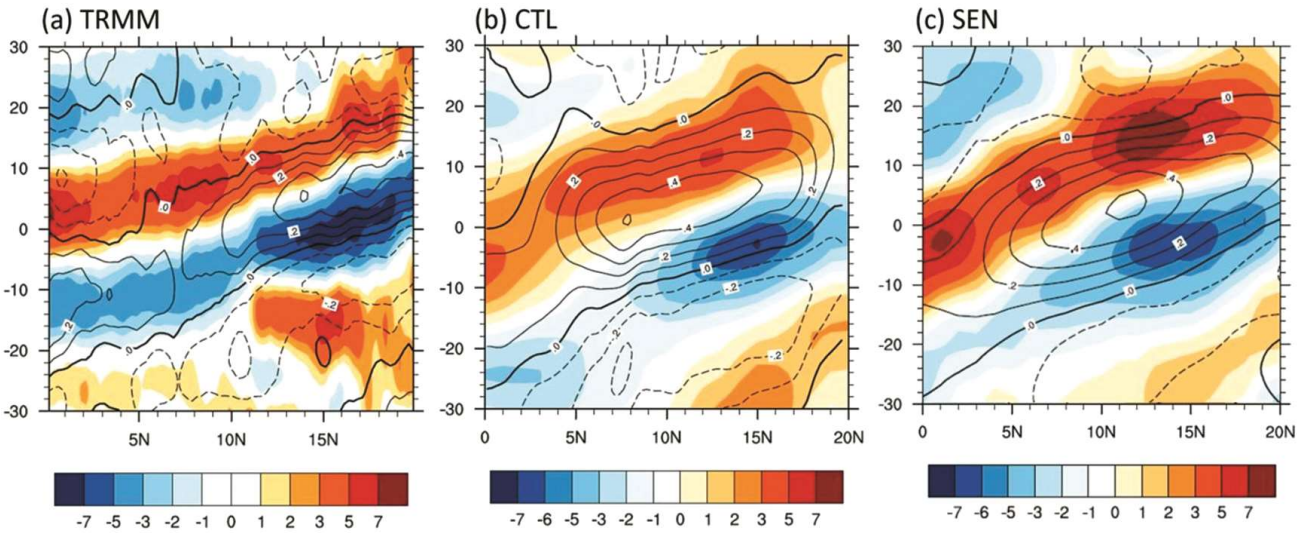

Fig. 5 — Hovmöller diagrams for filtered rainfall anomalies (mm/day; coloured shading) and SST anomalies (°C; contours) in (a) Observation, (b) CTL, and (c) SEN run. The anomalies are averaged longitudinally over 85° E – 95° E. The horizontal axis represents the latitude, and the vertical axis represents the number of days prior to (negative) and after (positive) the peak of the break phase over central India (CI)

anomalies averaged over the central Indian box. *i.e.*, 15° N – 25° N, 70° E – 85° E. The active (break) phase of the monsoon is defined as the days when the MISO index is greater (smaller) than +1 (-1). MISOs start near the south of the equator and propagate northward all the way to 20° N. Hovmöller analysis of rainfall anomalies associated with MISO northward propagation is carried out during the break phase (-30 to 30 days of peak break day) over BoB. Figure 5 shows the observed and model-simulated longitudinally (85°:95° E) averaged filtered rainfall (shading) and SST (contour) anomalies during the break phase of the monsoon. In observation and model simulations, northward propagation of negative rainfall anomalies followed by positive anomalies indicates that an active phase follows the break phase. In observation, the anomalies start near the equator, propagate up to 20° N, and are stronger during the active phase following the break phase. However, in the CTL run, the MISO rainfall anomalies during active and break phases are significantly weaker than those observed. Also, the propagation of rainfall anomalies is restricted to a latitude of 16° N. On the other hand, SEN simulation shows an improved MISO northward propagation in terms of both stronger magnitude and farther location of northward propagation of rainfall anomalies. Cooler SST anomalies prior to the break phase and warmer SST anomalies prior to the active phase can be seen in observation, and model simulations are in line with earlier studies. The warmer SST anomalies before the active spell (and during the break spell) destabilise the lower atmosphere and enhance convection[50,51]. The underestimation of rainfall anomalies in CTL is also associated with weaker SST response during the break phase and following the active phase. Further comparison of SST anomalies in the model simulations indicates that warmer SSTs prior to the active phase are stronger in the SEN run (~0.6 °C) compared to the CTL run (~0.4 °C). Therefore, warmer SST anomalies in the SEN run destabilise the atmosphere more than the CTL; hence, the precipitation anomalies during the active spell are also stronger in the SEN run. Including diurnal SST and flux parameterisation also improves the SST response during MISO northward propagation in the SEN run.

At the intra-seasonal scale, surface heat flux (Q_{net}) and mixed layer dynamics drive the intra-seasonal SST changes during the coupled evolution and northward propagation of monsoon intra-seasonal oscillations[50-53]. Therefore, an analysis similar to the earlier figure is carried out to compare the Q_{net} and MLD variability during and after the monsoon break in observation and model simulations, as shown in Figure 6. The comparison of CTL and SEN simulations can point out the dynamic impact of the diurnal scale on the intra-seasonal scale. In both reanalysis and model simulations, Q_{net} leads to SST anomalies by approximately ten days. A similar lead-lag between Q_{net} and SST was also observed by

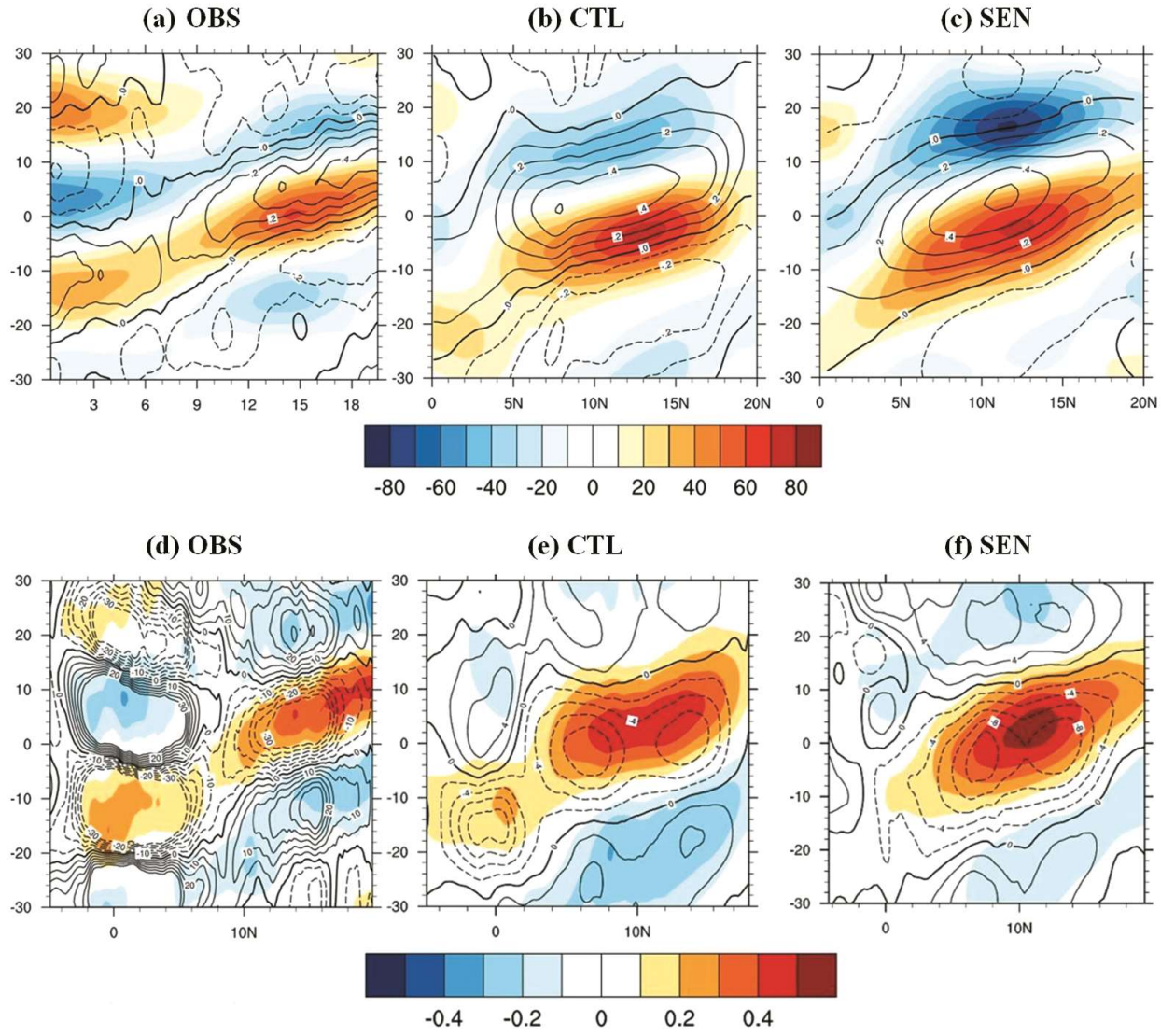

Fig. 6 — Hovmöller diagrams for filtered Q_{net} (Wm^{-2}; shading) and SST anomalies (°C; contours) in (a) OBS, (b) CTL, and (c) SEN run. (d - f) same as (a - c) but for filtered SST (°C; shading) and MLD (m; contour) anomalies. The anomalies are averaged longitudinally over 85° E – 95° E. The axes are the same as mentioned in Figure 5

Sengupta *et al*.[50]. Hence, they concluded that the SST anomalies are basically generated by surface heat flux anomalies, which modulate the northward propagating active/break phase in convection. The break (active) phase of the monsoon is characterised by weaker (stronger) winds, which reduce (enhance) the turbulent flux from the ocean surface[16,50]. The comparison of model simulations suggests that the Q_{net} anomalies are amplified in the SEN run during and after the break phase compared to the CTL run. The reduction in latent heat flux (figure not shown) in the SEN run results in a higher Q_{net} and warmer SST anomalies before the subsequent active phase. The modified surface heat flux with warmer SST can modulate the moist static energy budget[51] to favour enhanced convection. Due to well-organised and enhanced convection, the subsequent active phase is accompanied by a stronger precipitation anomalies. During the active phase, the Q_{net} anomalies are reduced in the SEN run compared to the CTL run, indicating a stronger active phase. The convective downdrafts associated with a stronger active phase in the SEN run can cause a drier boundary layer and cooler surface air[15]. Hence, it increases the air-sea temperature and humidity difference, enhancing air-sea interactive fluxes such as the latent heat flux and

sensible heat flux. The stronger winds (not shown) during a convective period can result in higher air-sea fluxes. Whether the sub-surface ocean dynamics support similar inferences or not, further analysis on MLD is carried out. Figure 6(d - f) shows the MLD anomalies as contours with SST anomalies as coloured shading for reanalysis, CTL, and SEN runs. Shallower (deeper) MLD anomalies are found to be coherent with warmer (cooler) SST anomalies, although MLD anomalies slightly (by a few days) lead to the SST anomalies. The deeper (shallower) MLD anomalies prior to (during) the break phase are significantly stronger in GLORYS reanalysis than both CTL and SEN simulations. The MLD anomalies during the warming period/break phase (prior to the active phase) are shallower in the SEN run compared to the CTL run. Similarly, deeper MLD anomalies with cooler SSTs in the SEN run can be seen during the active phase. Therefore, it is evident that due to the rectification of intra-seasonal variability by the diurnal scale, both the surface, subsurface oceanic, and atmospheric conditions favour a strong break phase followed by a stronger active phase in the SEN run compared to the CTL run.

Addressing seasonal problems

As mentioned earlier, most of the global coupled models have significant problems in simulating seasonal mean rainfall patterns and their magnitude around the globe. Most of the coupled models overestimate (underestimate) the rainfall over the tropical oceanic (land) regions[19,23]. The present section discusses the cumulative impact of diurnal and intra-seasonal improvements due to the implementation of skin temperature and flux parameterisation on some of the mean biases causing hindrance to seasonal predictability in CFSv2. Figure 7 shows the seasonal mean rainfall bias in both model simulations. In the CTL run, the oceanic wet bias over the tropical Indo-Pacific Ocean is in the order of magnitude of 4 – 6 mm/day. SEN run significantly reduces wet bias over the tropical oceans, which is 3 – 5 mm/day. The dry bias over the tropical landmasses, specifically over India and South

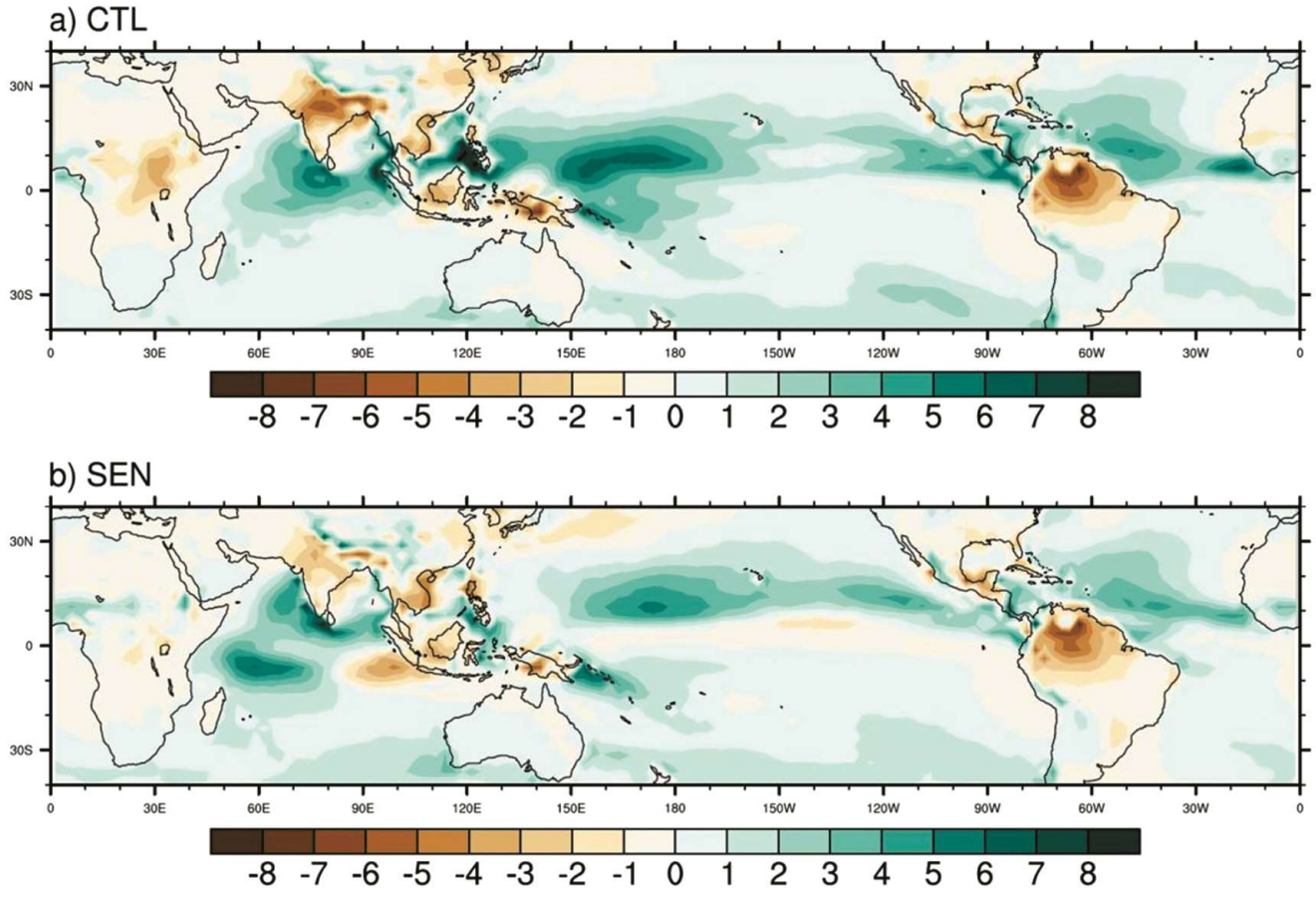

Fig. 7 — Seasonal (JJAS) mean rainfall bias (mm/day) in (a) CTL, and (b) SEN run

America, is of the order of 5 – 7 mm/day in the CTL run. In the SEN run, the dry bias over the Indian landmass is reduced by 2 – 4 mm/day. The reduction in dry bias in the SEN run can be attributed to (a) amplified diurnal rainfall activities, and (b) a stronger active phase of monsoon, as discussed in earlier sections. During the monsoon season, a significant enhancement in convective rainfall over central India is also noticed in the SEN run as compared to the CTL run (Fig. S1). The enhanced convective rainfall can contribute significantly towards the reduction of the seasonal rainfall bias in the SEN run.

Proper representation of tropical teleconnections, such as the IOD-monsoon, ENSO-monsoon, etc., is key for seasonal monsoon prediction over India. Most of the present-generation coupled models face challenges in reproducing realistic monsoon-SST teleconnections over tropical oceans[24]. Overestimation of the impact of ENSO on monsoon and opposite IOD-monsoon relations to that in observation are major weaknesses of coupled models that need to be addressed. Pradhan *et al*.[24] have pointed out that the improper simulation of surface ocean-atmosphere (SST-surface flux) and subsurface-to-surface ocean (thermocline-SST) relations are major factors contributing to the improper tropical teleconnections in models. In this study, we look at these teleconnections in model simulations with and without the presence of the diurnal cycle of the ocean and COARE 3.0 flux parameterisation. Table S1 shows the observed and model-simulated correlation of ocean monitoring indices such as two poles (IODe and IODw) and Dipole Model Index (DMI) for IOD and Niño 3.4 index with all India land averaged rainfall (ISMR). In the CTL (-0.75) run, the impact of ENSO on IMSR is overestimated as compared to the observation, whereas, in the SEN run (-0.25), the overestimation is reduced significantly. On the other hand, the association of IOD is better reproduced in the SEN run than in the CTL run. The correct polarity of association between monsoon rainfall and SST over the eastern and western poles of IOD in the SEN run shows improvement compared to the CTL run, where the associations are opposite to those in observation. Therefore, the phase of tropical teleconnections is better represented when the diurnal cycle in the surface ocean is included in the model parameterisation.

Conclusions

Building upon earlier studies that suggested improving air-sea interaction in coupled models can reduce systematic biases and improve model performance, this study attempted to improve the accuracy in representing the SST and surface fluxes. Diurnal warm layer and cool skin temperature correction to the bulk ocean temperature is incorporated in the CFSv2 model to account for the diurnal variability of the ocean surface. Also, the existing surface flux algorithm is replaced with the COARE 3.0 bulk flux algorithm to improve the accuracy of air-sea interactive fluxes. Analyses are performed to showcase how diurnal to seasonal scale challenges using the coupled model as a prediction/forecasting tool can be overcome through these revised model parameterisations. The diurnal scale analysis and comparison of model sensitivity experiments indicate that in the absence of skin temperature parameterisation, SST and MLD's diurnal phase and amplitude are not realistically reproduced in model simulations. However, implementing skin temperature parameterisation led to an improved representation of the timing of minima/maxima and diurnal range in SST and MLD in model simulations. The spatio-temporal diurnal characteristics of tropical precipitation are also significantly improved with the modified model configuration. The diurnal warming in the model triggered more convection; hence, the sensitivity simulations enhanced the diurnal range of tropical precipitation. This study also addressed the long-existing problem of weaker and slower northward propagating monsoon intra-seasonal rainfall anomalies in the coupled models. In the modified model, an enhanced diurnal warming with a shallower MLD during the break phase of the monsoon led to higher SST anomalies. This resulted in stronger moisture convergence and enhanced rainfall anomalies during the active phase following the break phase of the monsoon. The northward propagation characteristics are significantly better because of the improvements in diurnal warming-SST-precipitation response. The cumulative impact of the diurnal and intra-seasonal ocean, atmosphere, and air-sea boundary state resulted in the reduction of seasonal mean rainfall biases in the model. Specifically, the dry bias over Indian landmass is significantly reduced due to enhancement in diurnal and intra-seasonal precipitation characteristics over the oceanic regions. The present study also showcased

that the inability of the models to simulate a realistic ENSO-ISMR and IOD-ISMR can also be overcome to a certain extent with the diurnal skin temperature parameterisation and revised surface flux algorithm. Therefore, the study attempted to address the long-existing coupled model problems at diurnal, intra-seasonal, and seasonal time scales by improving the representation of the diurnal surface ocean and its scale interaction into a longer time scale.

Supplementary Data

Supplementary data associated with this article is available in the electronic form at https://nopr.niscpr.res.in/jinfo/ijms/IJMS_53(05)384-397_SupplData.pdf

Acknowledgments

We thank the Indian Institute of Tropical Meteorology, Ministry of Earth Sciences, India and Indian Institute of Technology, Bombay, India for making the resources available for carrying out the research work.

Conflict of Interest

Authors declare no competing or conflict of interest.

Ethical Statement

This research was conducted in accordance with ethical standards set by Ministry of Earth Sciences, Government of India. The manuscript was prepared according to the guidelines provided by Indian Journal of Geo-Marine Sciences. All authors provided informed consent before participation. Any potential conflicts of interest have been disclosed.

Author Contributions

MP conceptualised the study and conducted formal analyses. SAR & AB supervised the analyses and contributed to writing the original manuscript draft.

References

1 Sakamoto T T, Komuro Y, Nishimura T, Ishii M, Tatebe H, *et al.*, MIROC4h — A New High-Resolution Atmosphere-Ocean Coupled General Circulation Model, *J Meteor Soc Japan, Ser II*, 90 (3) (2012) 325–359. https://doi.org/10.2151/jmsj.2012-301

2 Oouchi K, Yoshimura J, Yoshimura H, Mizuta R, Kusunoki S, *et al.*, Tropical Cyclone Climatology in a Global-Warming Climate as Simulated in a 20 km-Mesh Global Atmospheric Model: Frequency and Wind Intensity Analyses, *J Meteor Soc Japan, Ser II*, 84 (2006) (2) 259–276. https://doi.org/10.2151/jmsj.84.259

3 Ramu D A, Sabeerali C T, Chattopadhyay R, Nagarjuna Rao D, George G, *et al.*, Indian summer monsoon rainfall simulation and prediction skill in the CFSv2 coupled model: Impact of atmospheric horizontal resolution, *J Geophys Res Atmos*, 121 (5) (2016) 2205–2221. https://doi.org/10.1002/2015JD024629

4 Ganai M, Krishna R P M, Mukhopadhyay P & Mahakur M, The impact of revised simplified Arakawa-Schubert scheme on the simulation of mean and diurnal variability associated with active and break phases of Indian summer monsoon using CFSv2, *J Geophys Res Atmos*, 121 (16) (2016) 9301–9323. https://doi.org/10.1002/2016JD025393

5 Sujith K, Saha S K, Rai A, Pokhrel S, Chaudhari H S, *et al.*, Effects of a multilayer snow scheme on the global teleconnections of the Indian summer monsoon, *QJR Meteorol Soc*, 145 (720) (2019) 1102–1117. https://doi.org/10.1002/qj.3480

6 Simmons H L, Jayne S R, St. Laurent L C & Weaver A J, Tidally driven mixing in a numerical model of the ocean general circulation, *Ocean Model*, 6 (3–4) (2004) 245–263.

7 Jung T, Balsamo G, Bechtold P, Beljaars A C M, Köhler M, *et al*., The ECMWF model climate: Recent progress through improved physical parametrizations, *QJR Meteorol Soc*, 136 (650) (2010) 1145–60. http://doi.wiley.com/10.1002/qj.634

8 Lin P, Yang Z L, Wei J, Dickinson R E, Zhang Y, *et al.*, Assimilating multi-satellite snow data in ungauged Eurasia improves the simulation accuracy of Asian monsoon seasonal anomalies, *Environ Res Lett*, 15 (2020) p. 64033. https://doi.org/10.1088/1748-9326/ab80ef

9 Alves O, Balmaseda M A, Anderson D & Stockdale T, Sensitivity of dynamical seasonal forecasts to ocean initial conditions, *QJR Meteorol Soc*, 130 (2004) 647–667. https://doi.org/10.1256/qj.03.25

10 Gade S V, Sreenivas P, Rao S A, Srivastava A & Pradhan M, Impact of the Ensemble Kalman Filter Based Coupled Data Assimilation System on Seasonal Prediction of Indian Summer Monsoon Rainfall, *Geophys Res Lett*, 49 (15) (2022) 1-11. https://doi.org/10.1029/2021GL097184

11 Balmaseda M & Anderson D, Impact of initialization strategies and observations on seasonal forecast skill, *Geophys Res Lett*, 36 (2009) 1–5. https://doi.org/10.1029/2008GL035561

12 Chakraborty A & Krishnamurti T N, Improved forecasts of the diural cycle in the tropics using multiple global models, Part II: Asian summer monsoon, *J Clim*, 21 (2008) 4045–4067. https://doi.org/10.1175/2008JCLI2107.1

13 Xie S, Wang Y C, Lin W, Ma H Y, Tang Q, *et al*., Improved Diurnal Cycle of Precipitation in E3SM With a Revised Convective Triggering Function, *J Adv Model Earth Syst*, 11 (7) (2019) 2290-2310. https://doi.org/10.1029/2019MS001702

14 Dai A & Trenberth K E, The Diurnal Cycle and Its Depiction in the Community Climate System Model, *J Clim*, 17 (2004) 930–951. https://doi.org/10.1175/1520-0442(2004)017<0930:TDCAID>2.0.CO;2

15 Chen S S & Houze R A, Diurnal variation and life-cycle of deep convective systems over the tropical pacific warm pool, *QJR Meteorol Soc*, 123 (1997) 357–88. https://doi.org/10.1002/QJ.49712353806

16 Li Y, Han W, Wang W, Zhang L & Ravichandran M, The Indian summer monsoon intraseasonal oscillations in CFSv2

forecasts: Biases and importance of improving air-sea interaction processes, *J Clim*, 31 (2018) 5351–5370. https://doi.org/10.1175/JCLI-D-17-0623.1

17 Sharmila S, Pillai P A, Joseph S, Roxy M, Krishna R P M, *et al*., Role of ocean-atmosphere interaction on northward propagation of Indian summer monsoon intra-seasonal oscillations (MISO), *Clim Dyn*, 41 (2013) 1651–1669. https://doi.org/10.1007/s00382-013-1854-1

18 Klingaman N P & Woolnough S J, The role of air–sea coupling in the simulation of the Madden–Julian oscillation in the Hadley Centre model, *QJR Meteorol Soc*, 140 (2014) 2272–86, https://doi.org/10.1002/QJ.2295

19 Sperber K R, Annamalai H, Kang I S, Kitoh A, Moise A, *et al*., The Asian summer monsoon: An intercomparison of CMIP5 vs. CMIP3 simulations of the late 20th century, *Clim Dyn*, 41 (2013) 2711–2744. https://doi.org/10.1007/s00382-012-1607-6

20 Goswami B B, Deshpande M, Mukhopadhyay P, Saha S K, Rao S A, *et al*., Simulation of monsoon intraseasonal variability in NCEP CFSv2 and its role on systematic bias, *Clim Dyn*, 43 (2014) 2725–2745.

21 Pillai P A, Rao S A, Srivastava A, Ramu D A, Pradhan M, *et al.*, Impact of the tropical Pacific SST biases on the simulation and prediction of Indian summer monsoon rainfall in CFSv2, ECMWF-System4, and NMME models, *Clim Dyn*, 56 (2021) 1699–1715. https://doi.org/10.1007/s00382-020-05555-1

22 Pillai P A, Rao S A, Ramu D A, Pradhan M & George G, Seasonal prediction skill of Indian summer monsoon rainfall in NMME models and monsoon mission CFSv2, *Int J Clim*, 38 (2018) e847–e861. https://doi.org/10.1002/joc.5413

23 Pradhan M, Rao S A, Doi T, Pillai P A, Srivastava A, *et al.*, Comparison of MMCFS and SINTEX-F2 for seasonal prediction of Indian summer monsoon rainfall, *Int J Clim*, 14 (13) (2021) 6084-6108. https://doi.org/10.1002/joc.7169

24 Pradhan M, Yadav R K, Ramu Dandi A, Srivastava A, Phani M K, *et al.*, Shift in MONSOON–SST teleconnections in the tropical Indian Ocean and ENSEMBLES climate models' fidelity in its simulation, *Int J Clim*, 37 (2017) 2280–2294. https://doi.org/10.1002/joc.4841

25 Neelin J D, Battisti D S, Hirst A C, Jin F-F, Wakata Y, *et al.*, ENSO theory, *J Geophys Res Ocean*, 103 (1990) 14261–14290. https://doi.org/10.1029/97JC03424

26 Swain D & Ghose S K, Latent and Sensible heat flux variation in north Indian Ocean during ENSO and Indian Ocean dipole years, In: *33rd General Assembly and Scientific Symposium of the International Union of Radio Science*, *URSI GASS*, Rome, Italy, 29 August 2020 – 05 September 2020, 2020, pp. 1-3. https://doi.org/10.23919/URSIGASS49373.2020.9232005

27 Saji N H, Goswami B N, Vinayachandran P N & Yamagata T, A dipole mode in the tropical Indian Ocean, *Nature*, 401 (1999) 360–363. https://doi.org/10.1038/43854

28 Madden R A &n Julian P R, Detection of a 40–50 Day Oscillation in the Zonal Wind in the Tropical Pacific, *J Atmos Sci*, 28 (1971) 702–708. https://doi.org/10.1175/1520-0469(1971)028<0702:doadoi>2.0.co;2

29 Webster P J & Lukas R, TOGA COARE: The Coupled Ocean–Atmosphere Response Experiment, *Bull Am Meteteorol Soc*, 79 (9) (1992) 1377–1416. https://doi.org/10.1175/1520-0477(1992)073%3C1377:TCTCOR%3E2.0.CO;2

30 Mallick S K, Agarwal N, Sharma R, Prasad K V S R & Ramakrishna S S V S, Thermodynamic Response of a High-Resolution Tropical Indian Ocean Model to TOGA COARE Bulk Air–Sea Flux Parameterization: Case Study for the Bay of Bengal (BoB), *Pure Appl Geophys*, 177 (2020) 4025–4044. https://doi.org/10.1007/s00024-020-02448-6

31 Misra V, Marx L, Brunke M & Zeng X, The equatorial pacific cold tongue bias in a coupled climate model, *J Clim*, 21 (2008) 5852–5869. https://doi.org/10.1175/2008JCLI2205.1

32 Zhang R, Zhou F, Wang X, Wang D & Gulev S K, Cool Skin Effect and its Impact on the Computation of the Latent Heat Flux in the South China Sea, *J Geophys Res Oceans*, 126 (1) (2021) p. 2020JC016498. https://doi.org/10.1029/2020JC016498

33 Rao S A, Goswami B N, Sahai A K, Rajagopal E N, Mukhopadhyay P, *et al*., Monsoon Mission: A targeted activity to improve monsoon prediction across scales, *Bull Am Meteorol Soc*, 100 (12) (2019) 2509–2532.

34 Saha S, Moorthi S, Wu X, Wang J, Nadiga S, *et al*., The NCEP climate forecast system version 2, *J Clim*, 27 (2014) 2185–2208. https://doi.org/10.1175/JCLI-D-12-00823.1

35 Large W G & Yeager S G, Diurnal to decadal global forcing for ocean and seaice models: The data sets and flux climatologies, NCAR Tech Notes, TN/460+STR, 2004, pp. 105.

36 Zeng X, Zhao M & Dickinson R E, Intercomparison of bulk aerodynamic algorithms for the computation of sea surface fluxes using TOGA COARE and TAO data, *J Clim*, 11 (1998) 2628–2644. https://doi.org/10.1175/1520-0442(1998)011<2628:IOBAAF>2.0.CO;2

37 Brunke M A, Uncertainties in sea surface turbulent flux algorithms and data sets, *J Geophys Res Ocean*, 107 (C10) (2002) 1-21. https://doi.org/10.1029/2001JC000992

38 Fairall C W, Bradley E F, Rogers D P, Edson J B & Young G S, Bulk parameterization of air-sea fluxes for Tropical Ocean-Global Atmosphere Coupled-Ocean Atmosphere Response Experiment, *J Geophys Res Ocean*, 101 (C2) (1996) 3747-3764. https://doi.org/10.1029/95JC03205

39 Fairall C W, Bradley E F, Hare J E, Grachev A A & Edson J B, Bulk parameterization of air-sea fluxes: Updates and verification for the COARE algorithm, *J Clim*, 16 (2003) 571–591. https://doi.org/10.1175/1520-0442(2003)016<0571:BPOASF>2.0.CO;2

40 Saha S, Moorthi S, Pan H-L, Wu X, Wang J, *et al*., NCEP climate forecast system reanalysis (CFSR) 6-hourly products, January 1979 to December 2010, Research Data Archive at the National Center for Atmospheric Research, Computational and Information Systems Laboratory, Boulder, CO, 2010. Accessed online at: https://cmr.earthdata.nasa.gov/search/concepts/C1214110933-SCIOPS.html

41 Slingo J, Inness P, Neale R, Woolnough S & Yang G, Scale interactions on diurnal to seasonal timescales and their relevance to model systematic errors, *Ann Geophys*, 46 (1) (2003) 139-155. https://doi.org/10.4401/ag-3383

42 Clayson C A & Chen A, Sensitivity of a Coupled Single-Column Model in the Tropics to Treatment of the Interfacial Parameterizations, *J Clim*, 15 (2002) 1805–1831.

https://doi.org/10.1175/1520-442(2002)015<1805:SOACSC>2.0.CO;2

43 Li W, Yu R, Liu H & Yu Y, Impacts of Diurnal Cycle of SST on the Intraseasonal Variation of Surface Heat Flux over the Western Pacific Warm Pool, *Adv Atmos Sci*, 18 (2001) 793–806. https://doi.org/10.1007/BF03403503

44 Bernie D J, Woolnough S J, Slingo J M & Guilyardi E, Modeling diurnal and intraseasonal variability of the ocean mixed layer, *J Clim*, 18 (2005) 1190–1202. https://doi.org/10.1175/JCLI3319.1

45 Shinoda T, Impact of the Diurnal Cycle of Solar Radiation on Intraseasonal SST Variability in the Western Equatorial Pacific, *J Clim*, 18 (2005) 2628–2636. https://doi.org/10.1175/JCLI3432.1

46 Bellenger H, Takayabu Y N, Ushiyama T & Yoneyama K, Role of Diurnal Warm Layers in the Diurnal Cycle of Convection over the Tropical Indian Ocean during MISMO, *Mon Weather Rev*, 138 (2010) 2426–2433. https://doi.org/10.1175/2010MWR3249.1

47 Brunke M A, Zeng X, Misra V & Beljaars A, Integration of a prognostic sea surface skin temperature scheme into weather and climate models, *J Geophys Res Atm*, 113 (D21) (2008) p. D21117. https://doi.org/10.1029/2008JD010607

48 Yan Y, Zhang L, Yu Y, Chen C, Xi J, *et al.*, Rectification of the Intraseasonal SST Variability by the Diurnal Cycle of SST Revealed by the Global Tropical Moored Buoy Array, *Geophys Res Lett*, 48 (2021) p. e2020GL090913. https://doi.org/10.1029/2020GL090913

49 Mujumdar M, Salunke K, Rao S A, Ravichandran M & Goswami B N, Diurnal cycle induced amplification of sea surface temperature intraseasonal oscillations over the bay of Bengal in summer monsoon season, *IEEE Geosci Remote Sens Lett*, 8 (2011) 206–210. https://doi.org/10.1109/LGRS.2010.2060183

50 Roxy M & Tanimoto Y, Role of SST over the Indian Ocean in influencing the intraseasonal variability of the Indian summer monsoon, *J Meteorol Soc Japan Ser II*, 85 (3) (2007) 349-358. https://doi.org/10.2151/jmsj.85.349

51 Shinoda T, Hendon H H & Glick J, Intraseasonal Variability of Surface Fluxes and Sea Surface Temperature in the Tropical Western Pacific and Indian Oceans, *J Clim*, 11 (1998) 1685–1702. https://doi.org/10.1175/1520-0442(1998)011

52 Kemball-Cook S & Wang B, Equatorial waves and air-sea interaction in the boreal summer intraseasonal oscillation, *J Clim*, 14 (2001) 2923–2942. https://doi.org/10.1175/1520-0442(2001)014<2923:EWAASI>2.0.CO;2

53 Curry J A, Bentamy A, Bourassa M A, Bourras D, Bradley E F, *et al*., SEAFLUX, *Bull Am Meteorol Soc*, 85 (2004) 409–424. https://doi.org/10.1175/BAMS-85-3-409

54 Huffman G J, Adler R F, Bolvin D T & Nelkin E J, The TRMM Multi-Satellite Precipitation Analysis (TMPA), In: *Satellite Rainfall Applications for Surface Hydrology*, 1st edn, edited by Gebremichael M & Hossain F, (Springer, Dordrecht), 2010, 3–22. https://doi.org/10.1007/978-90-481-2915-7_1

55 McPhaden M J, Connell K J, Foltz G R, Perez R C & Grissom K, Tropical Ocean Observations for Weather and Climate: A Decadal Overview of the Global Tropical Moored Buoy Array, *Oceanography*, 36 (2-3) (2023) 32-43. https://doi.org/10.5670/oceanog.2023.211

56 Adler R, Sapiano M, Huffman G, Wang J-J, Gu G, *et al*., The Global Precipitation Climatology Project (GPCP) Monthly Analysis (New Version 2.3) and a Review of 2017 Global Precipitation, *Atmosphere (Basel)*, 9 (4) (2018) p. 138. https://doi.org/10.3390/atmos9040138

57 Huang B, Thorne P W, Banzon V F, Boyer T, Chepurin G, *et al*., Extended Reconstructed Sea Surface Temperature, Version 5 (ERSSTv5): Upgrades, Validations, and Intercomparisons, *J Clim*, 30 (2017) 8179–8205. https://doi.org/10.1175/JCLI-D-16-0836.1

58 Kumar B P, Vialard J, Lengaigne M, Murty V S N & McPhaden M J, TropFlux: Air-sea fluxes for the global tropical oceans-description and evaluation, *Clim Dyn*, 38 (2012) 1521–1543. https://doi.org/10.1007/s00382-011-1115-0

59 Kobayashi S, Ota Y, Harada Y, Ebita A, Moriya M, *et al*., The JRA-55 reanalysis: General specifications and basic characteristics, *J Meteorol Soc Japan*, 93 (1) (2015) 5-48. https://doi.org/10.2151/jmsj.2015-001

60 Jean-Michel L, Eric G, Romain B B, Gilles G, Angélique M, *et al*., The Copernicus Global 1/12° Oceanic and Sea Ice GLORYS12 Reanalysis, *Front Earth Sci (Lausanne)*, 9 (2021) p. 698876. https://doi.org/10.3389/feart.2021.698876